Positive Lyapunov exponents calculated from time series of strange nonchaotic attractors

Jian-Wei Shuai,* Jun Lian, Philip J. Hahn, and Dominique M. Durand
Department of Biomedical Engineering, Case Western Reserve University, Cleveland, Ohio 44106
(Received 30 January 2001; published 23 July 2001)

Time-series methods for estimating Lyapunov exponents may give a positive exponent when they are applied to the time series of strange nonchaotic systems. Strange nonchaotic systems are characterized by expanding and contracting regions in phase space that result in repeatedly expanding or contracting trajectories. Using time-series methods, the maximum time-series Lyapunov exponent is calculated as an average of the locally most expanding exponents that characterize the divergence of nearby trajectories following a reconstructed attractor over time. A positive exponent is reported by time-series methods for trajectories in an expanding region. While in a converging region, the most expanding dynamics are related to the quasiperiodic driving force. Statistically, a zero exponent related to the quasiperiodic force is obtained through time-series methods within converging regions. As a result, the calculated maximum Lyapunov exponent is positive.

DOI: 10.1103/PhysRevE.64.026220 PACS number(s): 05.45.−a

I. INTRODUCTION

The Lyapunov exponent is an important parameter for the analysis of nonlinear systems. It provides a quantitative measure of the sensitivity of a system to perturbations of initial conditions. Calculation of the Lyapunov spectrum permits estimation of the fractal dimension and Kolmogorov entropy of an attractor. In most practical situations where details of the dynamics of a system are not known, the only available information is the time series of a scalar quantity. Time-series data may be used to obtain a reconstructed attractor that retains information on the dynamics of the system [1–5]. Different algorithms have been proposed for the determination of Lyapunov exponents from a time series alone [6–13]. For clarity, in this paper the measure is termed original Lyapunov exponent (OLE) Λ^{O} when it is calculated from the equations of the original system and time-series Lyapunov exponent (TSLE) Λ^{TS} when it is calculated from a time series using time-series methods.

Many factors are involved in obtaining an accurate TSLE. First, the reconstructed attractor in time-delay coordinate space should be topologically equivalent to the original attractor of the system [1,3,5]. There are many discussions on how to determine the correct embedding, dimension and time-delay parameters [6,10,11,14]. Spurious TSLEs can be obtained with an inappropriate embedding dimension [15] Recording precision, the overall length of data used, the fractal character of the data, and noise characteristics also affect the accuracy of the TSLE value obtained [6,10–13,16]. As a special example, consider that a positive TSLE can be obtained for a random time series [17]. For each TSLE method there are also some adjustable parameters that affect the TSLE. These include factors such as how the neighbors are selected and how often the nearby trajectories are renormalized [6–13].

*Corresponding author: Department of Physics and Astronomy, Clippinger Research Laboratories, Room 252A, Ohio University, Athens, OH 45701. FAX: 740 593 0433. Email address: shuai@helios.phy.ohiou.edu

Currently, time-series methods are proposed mainly for autonomous systems. But in practice, they are widely applied to complex systems that may be nonautonomous. Strange nonchaotic attractors (SNA) represent one type of nonautonomous system. It is known that SNAs are geometrically complicated, but typical trajectories on these attractors exhibit no sensitive dependence on initial conditions asymptotically [18–24]. Because the properties of SNAs lie between order and chaos, an interesting question concerns whether time-series methods can distinguish SNA from chaos. In this paper we show that a positive TSLE can be obtained using time-series methods for data from strange nonchaotic systems. This observation, a positive TSLE for SNA, is explained by the mixing of eigendirections in tangent space by the time-series methods.

II. QUASIPERIODICALLY DRIVEN LOGISTIC MAP

Quasiperiodically driven logistic maps are discussed in this section (ω irrational):

$$x_{n+1}=f(x_n,\phi_n), \tag{1}$$

$$\phi_{n+1}=\phi_n+2\pi\omega \mod 2\pi. \tag{2}$$

Here x_n and ϕ_n are the state of the map and phase angle of the driving force at time n, respectively. These maps are two dimensional and therefore have two OLEs. Related to Eq. (1) there is a nontrivial OLE given by

$$\Lambda^{\mathrm{O}}=\lim_{N\to\infty}\frac{1}{N}\sum_{n=1}^{N}\ln\left|\frac{\partial f}{\partial x_n}\right|. \tag{3}$$

A trivial OLE is related to Eq. (2).

Two SNA examples are considered. First we examine the following map:

$$f(x_n,\phi_n)=\alpha(1+\varepsilon\cos\phi_n)x_n(1-x_n), \tag{4}$$

where $\omega=(\sqrt{5}-1)/2$ and $\varepsilon=0.1$. Using this map, SNA is found in the range $3.2714<\alpha<3.274$ [19]. Time series from

TABLE I. Time-series Lyapunov exponent estimated with four methods for time series of chaotic attractor and torus attractor. Here time delay $T=1$.

	Chaotic attractor Embedding dimension				Torus attractor Embedding dimension			
Method	2	3	4	5	2	3	4	5
Wolf	0.088	0.071	0.071	0.071	0.000	0.000	0.000	0.000
Kantz		0.057~0.073				0.000		
Sona	0.480	0.074	0.066	0.112	0.060	0.000	0.000	0.000
Brown	1.063	0.061	0.061	0.061	0.027	0.000	0.000	0.000

the SNA obtained with $\alpha=3.273$ are used as a first example. Its nontrivial OLE is $\Lambda^{O}=-0.008$.

Four well known methods are used in this paper to estimate the maximum TSLE of the time series. Two of them, discussed by Wolf *et al.* [6] and Kantz [7] work in the phase space of the reconstructed attractor by estimating divergence of nearby states directly. The other two, discussed by Sano and Sawada [9] and Brown *et al.* [12], work in the tangent space of the reconstructed attractor by estimating local Jacobian matrices. In all simulations, data are recorded with a precision of 10^{-6} after ignoring the first 2000 data points. For Brown's method 8192 points are used. For the other three methods 10 000 points are used. With Brown's method, the order of the fitted polynomial function is three and the local and global dimensions are both equal to the embedding dimension.

The first step in the reconstruction of an attractor from a time series is to determine an appropriate time delay and embedding dimension. Strictly speaking, the embedding theories of Takens and Suaer *et al.* [1,3] are not valid for nonautonomous systems. Hence, one could argue that the quasiperiodically driven map [Eq. (4)] cannot be embedded. However, the special harmonic nature of the driving force allows the phase dynamics to be written in an autonomous manner [Eqs. (1) and Eq. (2)], involving an additional degree of freedom (a discrete time harmonic oscillator). The particular structure of lacking feedback from x to ϕ is sometimes denoted as a skew system. For discrete maps, the time delay $T=1$ is typically used [5,12]. The embedding dimension may be approximated by selecting various values and comparing TSLEs calculated to the OLE. Table I shows the results for Eq. (4) using four time series methods. For $\alpha=3.3$, the attractor is chaotic with $\Lambda^{O}=0.06$ and 0.0; for $\alpha=3.2$, the attractor is a torus with $\Lambda^{O}=0.0$ and -0.15. It can be seen that all four time-series methods can give a good estimation of maximum OLE for these two attractors with embedding dimension three or four. As we show later, determination of the exact value of the embedding dimension is not critical. Here we stress that, for the torus, the time-series methods report a zero TSLE, that is related to the quasiperiodic driving force, rather than the nontrivial movement of the logistic map.

Next we apply these four methods to the SNA time series. The resulting TSLEs are given in Table II, all of which are positive. A discussion on how to get an exact TSLE for a time series is not intended, rather we simply demonstrate that a positive TSLE can be obtained for time series of strange nonchaotic systems. By varying the embedding dimension from two to six and the time delay from one to four, we found that the sign of maximum TSLE is not sensitive to parameter selection. Disregarding the quantitative differences among the methods tested, we stress here that a consistent result, a positive value for maximum TSLE, is yielded by these four different time-series algorithms.

The practical importance of this finding is mainly related to the probability of finding a strange nonchaotic attractor in physical systems. Originally, it was suggested that SNAs occur only in a small region in the parameter space of quasiperiodically driven systems [18–22]. It is rare to find such attractors experimentally. However, recent studies have shown that SNAs can occur in a large region in the parameter space of low-frequency quasiperiodically driven systems [23,24]. Therefore, as a second SNA example, we examine the following map:

$$f(x_n,\phi_n)=\alpha x_n(1-x_n)+\varepsilon\cos\phi_n, \tag{5}$$

where $\omega=0.01+10^{-5}\cdot\sqrt{5}$ and $\varepsilon=0.12$. SNAs can be found in a large region of parameter space for this map [23]. As an example, for $\alpha=3.6$, an SNA is obtained with $\Lambda^{O}=-0.033$. We applied the four time-series methods to this SNA example. The results are given in Table III. It can be seen that the positive sign of the maximum TSLE obtained in each case is robust to variation of the embedding dimension in the range from two to six and time delay from one to four.

III. ORIGIN OF THE POSITIVE TSLE

The calculation of positive TSLEs using time-series methods on strange nonchaotic systems can be explained by the

TABLE II. Time-series Lyapunov exponent estimated with four methods for SNA time series given in Eq. (4). In the last column, the minimum and maximum TSLEs obtained are given for varying embedding dimension and time delay.

	Embedding dimension (time delay $T=1$)				Embedding dimension range: 2–6
Method	2	3	4	5	Time delay range: 1–4
Wolf	0.021	0.012	0.013	0.014	0.01–0.03
Kantz		0.020–0.070			0.02–0.07
Sona	0.420	0.020	0.021	0.052	0.01–0.42
Brown	0.663	0.024	0.025	0.018	0.02–0.70

TABLE III. Time-series Lyapunov exponent estimated with four methods for SNA time series given in Eq. (5). In the last column, the minimum and maximum TSLEs obtained are given for varying embedding dimension and time delay.

	Embedding dimension (time delay $T=1$)				Embedding dimension range: 2–6
Method	2	3	4	5	Time delay range: 1–4
Wolf	0.123	0.112	0.109	0.114	0.09–0.13
Kantz		0.080–0.250			0.06–0.26
Sona	0.240	0.092	0.101	0.183	0.09–0.25
Brown	0.236	0.278	0.279	0.274	0.13–0.28

mixing of eigendirections in tangent space. Consider the finite-time Lyapunov exponents (or local exponents) of the systems. The finite-time OLE of Eq. (1) for a small fixed observation window τ is given by

$$\lambda_\tau^{\mathrm{O}}(n_0)=\frac{1}{\tau}\sum_{n=n_0}^{n_0+\tau-1}\ln\left|\frac{\partial f}{\partial x_n}\right|. \tag{6}$$

The exponent $\lambda_\tau^{\mathrm{O}}(n_0)$ quantifies the expanding or contracting influence that the trajectory experiences from time n_0 to $n_0+\tau$ [23]. For a time series, the maximum TSLE is defined as an average over a long time of the locally most expanding exponents with respect to the motion of the reconstructed trajectory of data [5,6]. The finite-time TSLE $\lambda_\tau^{\mathrm{TS}}(n_0)$ can be calculated as the same average in the window from n_0 to $n_0+\tau$. Without loss of generality, Wolf's phase space method [6] is used as an example for calculating the finite-time TSLE. The same conclusion can be drawn for any other time series method working either in phase space or in tangent space. These methods are all based on the same original Lyapunov exponent method of calculating the divergence rate of nearby trajectories. The maximum OLE or TSLE for the attractor is just the average of the finite-time OLEs or TSLEs obtained from a sequence of nonoverlapping time windows over a long time.

In Figs. 1(a) and 1(b), the curves of $\lambda_\tau^{\mathrm{O}}(n)$ and $\lambda_\tau^{\mathrm{TS}}(n)$ versus time n with a fixed observation window τ are given for the two SNA examples above. Note that the main difference between $\lambda_\tau^{\mathrm{O}}(n)$ and $\lambda_\tau^{\mathrm{TS}}(n)$ is that $\lambda_\tau^{\mathrm{O}}(n)$ repeatedly undergoes deeply negative peaks, but $\lambda_\tau^{\mathrm{TS}}(n)$ does not. The negative peaks with $\lambda_\tau^{\mathrm{O}}(n)<\lambda_\tau^{\mathrm{TS}}(n)$ can be observed occassionally for the case of Eq. (4). The repeated deep negative values of $\lambda_\tau^{\mathrm{O}}(n)$, on average, are sufficient to guarantee a negative OLE Λ^{O} for the two nonchaotic attractors. The lack of deep negative spikes for $\lambda_\tau^{\mathrm{TS}}(n)$ results in a positive TSLE Λ^{TS}.

For Eq. (5), there are two eigendirections in tangent space, associated with the logistic map and periodic force. Driven by a quasiperiodic force, the trajectory of the logistic map frequently visits expanding or contracting regions during alternating time intervals. Corresponding to these dynamics, the eigenvalues, as well as the finite-time OLEs of the logistic map trajectory are sometimes positive and sometimes negative. For a nonchaotic attractor, contracting dynamics dominate, so that deep negative peaks in the finite-time OLE frequently occur. As shown in Figs. 2(a) and 2(b), the quasiperiodic force drives the trajectory repeatedly through the expanding and contracting regions once per driving period. During the long interval of contracting dynamics, a long piece of toruslike trajectory can be observed. The corresponding finite-time OLEs, shown with a dotted line in Fig. 2(c), are typically negative, and result in a negative OLE. In addition to this eigendirection, the system also has an independent eigendirection with trivial eigenvalues and so a zero finite-time OLE, corresponding to the quasiperiodic force. In Fig. 2(c) the horizontal line $x=0$ represents the trivial finite-time OLEs. In comparison, the dotted gray line shows that for our skew system, the maximum OLE is located in the trivial eigendirection and is not always related to the locally most expanding dynamics.

Now, consider a reconstructed trajectory $\{X_n\}$ in time-delay coordinates for an SNA time series (X_n is a vector). As for the original trajectory, the reconstructed trajectory $\{X_n\}$ repeatedly experiences expanding and contracting dynamics during each driving period. As shown in Fig. 2(b), in the region of expanding dynamics (region E), the trajectory is chaotic-like. In the region of contracting dynamics (region C), the trajectory is torus-like. Figure 2 also shows that there are two more transient regions: Regions TE and TC. The transient region TE is at the onset of the region of expanding dynamics and the trajectory diverges gradually from a toruslike orbit. The transient region TC is at the onset of the contracting dynamics and the trajectory converges gradually and becomes less chaoticlike.

For Wolf's method, the local TSLE is always related to the locally most expanding exponents for the convergence or divergence of the tracing trajectory $\{X_n\}$ and trajectories starting at nearby initial conditions in phase space [6]. In region E, the chaoticlike orbits suggest a divergence rate of nearby trajectories. The time series methods typically respond to the eigenvalues corresponding to the expanding trajectories of logistic map. Positive finite-time TSLEs are then correctly obtained, as shown in Fig. 2. In region TC, the chaoticlike orbits are driven to converge on toruslike orbits. Negative finite-time TSLEs are obtained upon calculating the convergence rate of nearby trajectories. In regions E and TC the time series-methods typically reflect the eigenvalues of the logistic map.

Time-series methods for Regions C and TE, however, behave differently. In region C, the trajectory $\{X_n\}$ looks more like a piece of torus because of the quasiperiodic force. Statistically, the nearby trajectories typically neither depart from

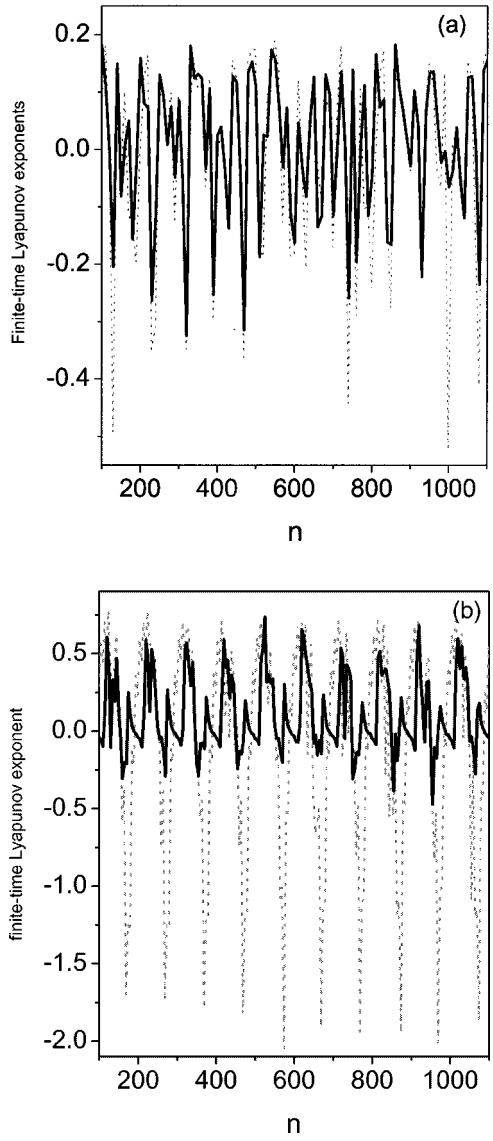

FIG. 1. Plots of the finite-time Lyapunov exponent $\lambda_\tau^{\mathrm{O}}(n)$ and $\lambda_\tau^{\mathrm{TS}}(n)$ versus time n with a fixed observation window for two SNA examples. (a) For SNA given by Eq. (4), here $\tau=10$. (b) For SNA given by Eq. (5), here $\tau=5$. The time is from 100 to 1100. Here $\lambda_\tau^{\mathrm{O}}(n)$ is drawn with a dotted gray line and $\lambda_\tau^{\mathrm{TS}}(n)$ is with a solid black line.

nor contract to the tracing trajectory $\{X_n\}$. The locally most expanding dynamics are then related to the trivial dynamics caused by the quasiperiodic driving force, rather than the nontrivial convergent dynamics of the logistic map. As a result, the time-series methods typically respond to the trivial eigenvalues of the periodic force in region *C*. On average, zero finite-time TSLEs are calculated for the pieces of toruslike trajectories (Fig. 2). This discussion is consistent with the observation that the TSLE is zero for a torus attractor, as shown in Table I. While in the transient region TE, although the original dynamics corresponding to the logistic map become expanding, the trajectories still remain toruslike for a while. As a result, zero finite-time TSLEs are still reported in region TE.

The behavior of the finite time TSLE suggest that there is

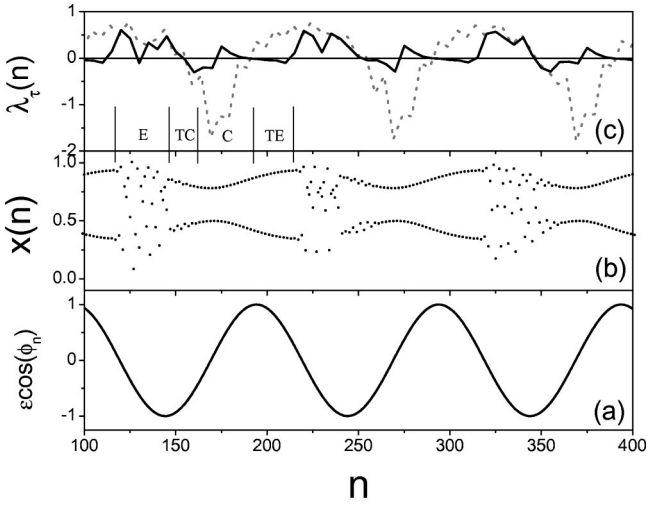

FIG. 2. The detailed trajectory and finite-time Lyapunov exponent for the SNA example given by Eq. (5). (a) The low-frequency quasiperiodically driving force. (b) The trajectory of the logistic map. (c) Plots of finite-time Lyapunov exponent $\lambda_\tau^{\mathrm{O}}(n)$ (given with the dotted line) and $\lambda_\tau^{\mathrm{TS}}(n)$ (given with the solid line) versus time n with a fixed observation window $\tau=5$. The x axis represents the trivial finite-time OLE. Here time is from 100 to 400. $\lambda_\tau^{\mathrm{O}}(n)$ is drawn with a dotted gray line and $\lambda_\tau^{\mathrm{TS}}(n)$ is with a solid black line. Four regions (*E*, TC, *C*, TE) are also roughly given in the figure.

a mixing effect of eigen-directions during calculation by time series methods. As a result, on average, positive TSLEs are obtained for region *E*, zero TSLEs for regions *C* and TE, and negative TSLEs for region TC. Due to its transient character, region TC should be relatively short. On the other hand, since strong expanding dynamics occur in region *E*, the attractor may become strange. If zero finite-time TSLEs are typically calculated in region *C*, the positive finite-time TSLEs in region *E* can then determine the fate of the averaged TSLE. A positive TSLE can be obtained for an SNA system by time series methods.

For the SNA example in Eq. (4), a repellor exists that is a continuous function of value ϕ in Eq. (2) [19]. Such a repellor is contained within the attractor. The attractor contacts the repellor in a countably dense set. The trajectories are frequently disturbed by the expanding dynamics. In this case, the time intervals for deeply contracting dynamics are typically short. Although the long pieces of region *C* and region *T* cannot be clearly observed for this attractor, the above discussion is still applicable. For this SNA, many short pieces of toruslike trajectory are created repeatedly over time. So, deeply negative peaks for exponents $\lambda_\tau^{\mathrm{O}}(n)$ can frequently occur, as shown in Fig. 1(a). Corresponding to the trivial eigenvalues of the periodic driving force, time-series methods typically report zero-approaching local TSLEs for these short toruslike pieces. As a result, the corresponding exponent $\lambda_\tau^{\mathrm{TS}}(n)$ does not reach the deep negative values. Due to the dense repellor, transient trajectories occur more frequently. For the trajectories within transient intervals between contracting dynamics and expanding dynamics, a small finite-time TSLE is likely to be calculated. However, because the systems discussed are nonchaotic, contracting

dynamics are dominant. If the mixing effect of eigendirections that results in zero finite-time TSLEs in the contracting region is strong, the positive finite-time TSLEs in region *E* can determine the sign of the averaged TSLE. As a result, a positive TSLE is obtained for an SNA.

IV. DISCUSSION AND CONCLUSION

In summary, we have shown that because of the mixing effect of eigendirections by the time-series methods a positive TSLE can be obtained for time-series from SNA systems. This result indicates that TSLE cannot be used as a parameter to distinguish SNA from chaos in experimental data. However, if other methods become available to identify time series as SNA or chaos, then a positive TSLE may be used to verify the SNA nature of the data.

The present time-series methods are mainly developed for autonomous systems, but are widely applied to complex nonautonomous systems in practice. For an autonomous system, the dynamics for any variable are always affected by the other variables. The maximum OLE is then always related to the locally most expanding dynamics over time. For a skew system or a nonautonomous system, the dynamics of some variables are independent of the others. The maximum OLE may not be always related to the locally most expanding dynamics over time. On the other hand, the maximum TSLE is always related to the locally most expanding dynamics of the reconstructed trajectory of the time series. So the maximum TSLE obtained is a good estimate of the maximum OLE for the autonomous system, but may not give a correct estimate of OLE for skew or nonautonomous systems.

ACKNOWLEDGMENT

The authors would like to thank J.Y. Chen for helpful discussion.

[1] F. Takens, in *Dynamical Systems and Turbulence*, edited by D. Rand and L.S. Young (Springer-Verlag, Berlin, 1981), p. 230.
[2] N.H. Packard, J.P. Crutchfield, J.D. Farmer, and R.S. Shaw, Phys. Rev. Lett. **45**, 712 (1980).
[3] T.D. Suaer, J.A. Yorke, and M. Casdagli, J. Stat. Phys. **65**, 579 (1991).
[4] J.-P. Eckmann and D. Ruelle, Rev. Mod. Phys. **57**, 617 (1985).
[5] H.D.I. Abarbanel, *Analysis of Observed Chaotic Data* (Springer-Verlag, New York, 1995).
[6] A. Wolf, J.B. Swift, H.L. Swinney, and J.A. Vastano, Physica D **16**, 285 (1985).
[7] H. Kantz, Phys. Lett. A **185**, 77 (1994).
[8] G. Paladin, M. Serva, and A. Vulpiani, Phys. Rev. Lett. **74**, 66 (1995).
[9] M. Sano and Y. Sawada, Phys. Rev. Lett. **55**, 1082 (1985).
[10] J.-P. Eckmann, S.O. Kamphorst, D. Ruelle, and S. Ciliberto, Phys. Rev. A **34**, 4971 (1986).
[11] P. Bryant, R. Brown, and H.D.I. Abarbanel, Phys. Rev. Lett. **65**, 1523 (1990).
[12] R. Brown, P. Bryant, and H.D.I. Abarbanel, Phys. Rev. A **43**, 2787 (1991).
[13] X. Zeng, R. Eykholt, and R.A. Pielke, Phys. Rev. Lett. **66**, 3229 (1991).
[14] M.B. Kennel, R. Brown, and H.D.I. Abarbanel, Phys. Rev. A **45**, 3403 (1992).
[15] T.D. Sauer, J.A. Tempkin, and J.A. Yorke, Phys. Rev. Lett. **81**, 4341 (1998).
[16] C. Rhodes and M. Morari, Phys. Rev. E **55**, 6162 (1997).
[17] T. Tanaka, K. Aihara, and M. Taki, Phys. Rev. E **54**, 2122 (1996).
[18] C. Grgbogi, E. Ott, S. Pelikan, and J.A. Yorke, Physica D **13**, 261 (1984).
[19] J.F. Heagy and S.M. Hammel, Physica D **70**, 140 (1994).
[20] A.S. Pikovsky and U. Feudel, Chaos **5**, 253 (1995).
[21] T. Yalcinkaya and Y.C. Lai, Phys. Rev. Lett. **77**, 5039 (1996).
[22] A. Prasad, V. Mehra, and R. Ramaswamy, Phys. Rev. Lett. **79**, 4127 (1997).
[23] J.W. Shuai and K.W. Wong, Phys. Rev. E **57**, 5332 (1998).
[24] J.W. Shuai, and K.W. Wong, Phys. Rev. E **59**, 5338 (1999).